Physics – Uspekhi **44** (11) 1199 – 1205 (2001)

CONFERENCES AND SYMPOSIA

PACS number: ?01.10.Fv

Scientific session of the Division of General Physics and Astronomy of the Russian Academy of Sciences (25 April 2001)

A scientific session of the Division of General Physics and Astronomy of the Russian Academy of Sciences (RAS) was held on 25 April 2001 at the P L Kapitza Institute for Physical Problems, RAS. The following reports were presented.

(1) **Aleksandrov E B** (S I Vavilov State Optical Institute, A F Ioffe Physico-Technical Institute, St. Petersburg) "Contemporary state of the techniques for measurements of the moduli of weak magnetic fields, from zero to ten oersted";

(2) **Sokolov I V** (St. Petersburg State University, V A Fok Institute of Physics, St. Petersburg), **Gatti A** (INFM, Dipartimento di Scienze CC FF MM, Università dell' Insubria, Como, Italy), **Kolobov M I** (Laboratoire PhLAM Université de Lille, Villeneuve d'Ascq, France), **Lugiato L A** (INFM, Dipartimento di Scienze CC FF MM, Università dell' Insubria, Como, Italy) "Quantum teleportation and holography";

(3) **Vartanyan T A** (S I Vavilov State Optical Institute, St. Petersburg) "Action of optical radiation on the boundary of a rarefied resonant medium. New possibilities and problems".

The reports presented are given below in brief.

PACS numbers: **06.20. – f**, 07.55.Ge
DOI: 10.1070/PU2001v044n11ABEH000987

Contemporary state of the techniques for measurements of the moduli of weak magnetic fields, from zero to ten oersted

E B Aleksandrov

Measurements of weak magnetic fields have many scientific and practical applications. Precision measurements of very weak fields (on the order of 1 μT) are of decisive importance in arranging certain fundamental experiments looking for violations of symmetry. For example, search for a constant neutron dipole moment currently calls for long-term (for 1000 s or so) stabilization of a weak magnetic field to an accuracy of no worse than 10 fT. The most relevant is the geomagnetic field range (20 – 80 μT), which is the domain of various geophysical studies, as well as diverse magnetic reconnaissance activities: ore exploration, archaeological research, military intelligence tasks, such as the detection of submarines and buried ammunition, search for sunken ships, installation of security perimeters, etc.

Today the best characteristics in the measurements of weak magnetic fields are achieved using so-called quantum magnetometers with the optical pumping of paramagnetic atoms or nuclei. Out of the many existing types we select those devices that possess a high sensitivity and absolute accuracy, as well as a quick response. These three characteristics are, to a certain extent, incompatible, and are best implemented in devices of different types. Special attention is paid to the recently developed M_x-potassium magnetometer with a narrow resonance line. This instrument is capable of covering the entire geomagnetic range, ensuring an exceptionally high sensitivity (on the order of 10 fT $Hz^{-1/2}$ in the band from 0.001 Hz and higher), with a reproducibility of readings as good as to 10 pT. Importantly, this device is of a quick-response type, allowing at least 10 readings per second. The absolute accuracy of measurements is formally determined by the accuracy of measurement of the gyromagnetic ratio and is of the order of 100 pT. An even better reproducibility of measurements is achieved in so-called tandems, which are combinations of a fast M_x magnetometer and a slow M_z magnetometer. The reproducibility of readings of a tandem is expected to be as good as 1 pT, and is apparently limited by the magnetic susceptibility of the structural materials. Today's methods of measurement of magnetic fields give a relative accuracy of 10^{-9} to 10^{-10}, which wins it the second place in metrology after frequency measurements.

Uspekhi Fizicheskikh Nauk **171** (11) 1263 – 1270 (2001)
Translated by A S Dobroslavskiĭ; edited by A V Getling

PACS number: **03.67. – a**
DOI: 10.1070/PU2001v044n11ABEH000995

Quantum teleportation and holography

I V Sokolov, A Gatti, M I Kolobov, L A Lugiato

Quantum teleportation allows the transfer of the quantum state of some system (for example, an electromagnetic field) from one point to another using the exchange of classical information in combination with a quantum channel that employs the quantum entangled states of auxiliary fields. One of the first phenomena of quantum information realized with optical methods was the quantum teleportation of spatially single-mode light beams. We demonstrate that the extension of the teleportation scheme to spatially multimode light beams makes it possible to teleport the quantum state of fields distributed in space and time — for example, fields carrying optical images. Such a form of teleportation (quantum holographic teleportation) may be regarded as the

ultimate case of holography with suppressed quantum noise and high-fidelity reproduction of the object field.

Quantum teleportation is one of the subjects of quantum information [1, 2], which has been developed especially fast since the early 1990s. It took only a few years to go from the first theoretical conjectures of certain phenomena of quantum information to their successful realizations, mainly by means of quantum optics. This was also made possible by the record-breaking experimental advances achieved in quantum optics with controlling light fields and atoms, in the sensitivity of detection, accuracy of measurements, etc.

The protocols of quantum teleportation rely considerably on the properties of entangled states. Assume, for example, that the quantum system is formed by two subsystems of the same physical nature (or differing in their physical nature but having formally similar sets of the basis states relevant in the given physical situation). Entangled states (or EPR states, for Einstein – Podolsky – Rosen) are those states of the system in which the individual observables of the subsystems exhibit the greatest uncertainty, whereas the mutually commuting observables that describe the relative state or motion of the subsystems are determined exactly. The EPR states are characterized by the ultimate quantum correlation of the constituent subsystems.

The first protocol of quantum teleportation was proposed in Ref. [3] for spin systems (the case of discrete variables). In optics, the analog of spin $1/2$ (in terms of similarity of the sets of basis states) is a single photon with two possible polarization states. Pure spin-$1/2$ states are associated with points on the sphere of spin directions, while the photon polarization states are represented by similar points on the Poincaré sphere. A source of EPR polarization states of two simultaneously emitted photons was created in Ref. [4] on the basis of spontaneous parametric scattering and was immediately used in an experimental realization of quantum teleportation [5], dense coding, and other protocols of quantum information. Subsequently, the quantum teleportation of continuous variables was proposed [6] and realized in an optical experiment [7], where a highly excited quantum state of a spatially single-mode light beam was teleported. The theory of quantum teleportation of a light field, spatially single-mode but broad-band in terms of frequency, was considered in Ref [8].

In this communication (see also Refs [9 – 11]), we discuss a more general version of the quantum teleportation of continuous variables, with a possibility of the high-fidelity teleportation of a quantum state of light fields distributed in both space and time. Interest in such an extension of the protocol of quantum teleportation is stimulated by the fact that such fields may be carriers of optical images, non-one-dimensional information arrays in parallel-data-processing schemes, etc. The indispensable part of the scheme in question (Fig. 1) as compared with the original scheme of Refs [6, 7] is a spatially distributed parallel quantum channel, which is realized with the use of spatially multimode EPR fields $E_1(\boldsymbol{\rho}, t)$ and $E_2(\boldsymbol{\rho}, t)$ that are in an entangled state. Here $\boldsymbol{\rho}$ is the coordinate in a transverse cross section of the beam.

Let us explain in plain terms the scheme of teleportation shown in Fig. 1, first without considering the EPR fields and their source (optical parametric amplifiers OPA_1, OPA_2, and the beam splitter BS_1). The object field $A_{\text{in}}(\boldsymbol{\rho}, t)$, whose quantum state is to be teleported, is scattered by the beam splitter BS_2 into two secondary beams, $B_x(\boldsymbol{\rho}, t)$ and $B_y(\boldsymbol{\rho}, t)$. This splitting is necessary for the subsequent optical mixing of

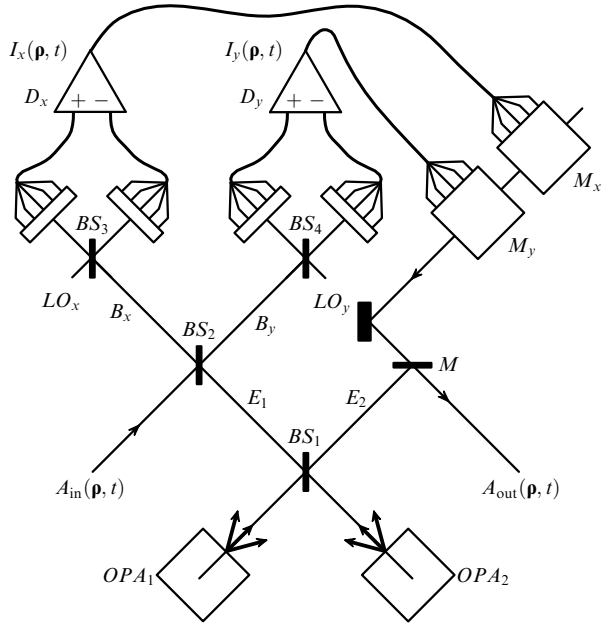

Figure 1. Scheme of quantum holographic teleportation.

each scattered wave with the strong classical reference wave (LO_x or LO_y) on the semitransparent mirror (BS_3 or BS_4). In the distributed light fields after each of these mirrors, a space – time signal is formed by the beats of the reference wave with the equiphase quadrature component of the object field. The phases of the reference waves are shifted by $\pi/2$, so that the two beat signals (one in the detection channel B_x and the other in B_y) together carry complete information about the field of the object wave. Differential detectors D_x and D_y are used to observe the space – time beat signals. The detector contains two matrices of effective photon counters (for example, CCD matrices), whose elements, for simplicity, are assumed to be small. The time-dependent surface densities of the photocurrents of the two matrices of each detector are subtracted. The signal from the detector, directed via the multichannel classical communication line to the device where the teleported field $A_{\text{out}}(\boldsymbol{\rho}, t)$ is to be prepared, is the time-dependent surface density of the differential current $I_x(\boldsymbol{\rho}, t)$ or $I_y(\boldsymbol{\rho}, t)$.

The classical signals produced in this way may be regarded as nonstationary holograms of the object field $A_{\text{in}}(\boldsymbol{\rho}, t)$. Indeed, they are formed through the same actions as used in recording holograms — optical mixing with a reference wave and the recording of the space beat signal. The analogy with holography is also present at the stage of preparation of the field $A_{\text{out}}(\boldsymbol{\rho}, t)$. The currents $I_x(\boldsymbol{\rho}, t)$ and $I_y(\boldsymbol{\rho}, t)$ control, with a space – time resolution, modulators M_x, M_y, which are illuminated by the reconstructing classical wave. In its quadrature amplitude of the reconstructing wave, each modulator creates a contribution that reproduces the time-dependent current density and eventually the corresponding quadrature amplitude of the input field $A_{\text{in}}(\boldsymbol{\rho}, t)$. Observe that the analogy between teleportation and holography was noted [12] even in the context of the teleportation of spatially single-mode fields.

The role of the quantum channel that converts holography into quantum holographic teleportation can be explained as follows. From the standpoint of classical optics, if there are no excited EPR fields $E_1(\boldsymbol{\rho}, t)$ and $E_2(\boldsymbol{\rho}, t)$, then there is no

field coming to the inputs of beam splitters BS_2 and M facing that direction. In a quantum description of this situation, however, we should take into account that the field oscillators of the waves illuminating these 'blank' inputs are in a vacuum state and carry an energy of $\hbar\omega/2$ per mode, where ω is the optical frequency. The notion of the spectral and angular energy densities of vacuum noise in free space can be obtained by associating the vacuum noise with thermal radiation at $k_B T \sim \hbar\omega$. This estimate gives the temperature T of the surface of the Sun.

It can be see from Fig. 1 that the vacuum field from input E_1 takes part in the recording and reconstruction of the dynamic hologram, as the field $A_{\text{in}}(\boldsymbol{\rho}, t)$ does, and introduces additional quantum fluctuations into the reconstructed field $A_{\text{out}}(\boldsymbol{\rho}, t)$. The independent vacuum field from input E_2 is mixed with the field $A_{\text{out}}(\boldsymbol{\rho}, t)$ on mirror M, whose reflectivity can be taken to be close to 1 (it can be demonstrated that, in any other configuration, a vacuum-noise input is also present). From the standpoint of quantum physics, it is these sources of fluctuations that set limits to the possibilities of reconstructing the object field in classical holography.

A rigorous description of the general case, where the scheme also involves a quantum channel (of EPR fields), relies on the concept of joint measurement in Bell's basis, conducted with the fields $A_{\text{in}}(\boldsymbol{\rho}, t)$ and $E_1(\boldsymbol{\rho}, t)$ in the left-hand part of Fig. 1. Here, however, one also can explain the physical nature and the role of entanglement, extending the known constructions (see, for example, Ref. [7]) to fields distributed in time and space.

One possible way to achieve the required entanglement consists in the optical mixing of fields $S_1(\boldsymbol{\rho}, t)$ and $S_2(\boldsymbol{\rho}, t)$ in a spatially multimode squeezed state [13–17]. These fields are generated in the optical parametric amplifiers OPA_1 and OPA_2, whose inputs receive fields in vacuum states $C_1(\boldsymbol{\rho}, t)$ and $C_2(\boldsymbol{\rho}, t)$. The squeezing transform written in a Fourier representation,

$$S_m(\boldsymbol{\rho}, t) \to s_m(\mathbf{q}, \Omega)\,, \qquad m = 1, 2$$

(and similarly for other fields), is

$$s_m(\mathbf{q}, \Omega) = U_m(\mathbf{q}, \Omega) c_m(\mathbf{q}, \Omega) + V_m(\mathbf{q}, \Omega) c_m^{\dagger}(-\mathbf{q}, -\Omega)\,, \quad (1)$$

where the coefficients $U_m(\mathbf{q}, \Omega)$, $V_m(\mathbf{q}, \Omega)$ are determined by the nonlinear susceptibility of the crystals, the pumping field strength, and the conditions of phase matching of waves. Further, we will consider collinear degenerate matching in type-I crystals. In Ref. [18], the possibility of obtaining two squeezed fields with orthogonal polarizations in a type-II nonlinear crystal was considered. The uncertainty regions for contributions to the fields $S_1(\boldsymbol{\rho}, t)$ and $S_2(\boldsymbol{\rho}, t)$ from harmonics with frequencies $\mathbf{q}, \Omega$ have the form of ellipses on the complex amplitude plane. The inclination of the major axis of the ellipse is

$$\psi_m(\mathbf{q}, \Omega) = \frac{1}{2} \arg\left\{ U_m(\mathbf{q}, \Omega) V_m(-\mathbf{q}, -\Omega) \right\}, \quad (2)$$

and the extension (squeezing) factor of the axes, $\exp\bigl(\pm r_m(\mathbf{q}, \Omega)\bigr)$, is given by the relationship

$$\exp\bigl(\pm r_m(\mathbf{q}, \Omega)\bigr) = \bigl|U_m(\mathbf{q}, \Omega)\bigr| \pm \bigl|V_m(\mathbf{q}, \Omega)\bigr|\,. \quad (3)$$

In order to obtain the EPR fields, the waves in the squeezed state should be phase-matched. We assume that the following conditions hold:

$$U_1(\mathbf{q}, \Omega) = U_2(\mathbf{q}, \Omega) \equiv U(\mathbf{q}, \Omega)\,,$$
$$V_1(\mathbf{q}, \Omega) = -V_2(\mathbf{q}, \Omega) \equiv V(\mathbf{q}, \Omega)\,. \quad (4)$$

Figures 2a and 2b show the uncertainty ellipses for the squeezed states of the fields $S_1(\boldsymbol{\rho}, t)$, $S_2(\boldsymbol{\rho}, t)$ at the exit of nonlinear crystals. The rotation of ellipses depending on the space frequency can be related to the diffraction of light waves in the course of nonlinear propagation and to the corresponding increase in the coherence area S_{c} of the light in the squeezed state; this eventually degrades the resolution of quantum holographic teleportation in space. The effects of diffraction, however, can be partly neutralized using a thin lens [13, 16]. Figures 2c and 2d show the uncertainty ellipses thus corrected.

The fields $E_1(\boldsymbol{\rho}, t)$ and $E_2(\boldsymbol{\rho}, t)$ in the entangled state can be obtained by mixing the fields $S_1(\boldsymbol{\rho}, t)$ and $S_2(\boldsymbol{\rho}, t)$ on the beam splitter BS_1:

$$E_n(\boldsymbol{\rho}, t) = \sum_{m=1,2} R_{nm} S_m(\boldsymbol{\rho}, t)\,, \quad (5)$$

where

$$\{R_{nm}\} = \frac{1}{\sqrt{2}} \begin{pmatrix} 1 & 1 \\ -1 & 1 \end{pmatrix} \quad (6)$$

is the scattering matrix of the splitter.

Figure 3 illustrates the emergence of correlations between the scattered fields. Consider the corresponding coherence volumes $V_{\text{c}} = cT_{\text{c}}V_{\text{c}}$ in the light fields in the squeezed state, incident on the mirror of the splitter. Here T_{c} is the coherence time. The uncertainty regions and the random local values of the field strength in these volumes are shown in the bottom

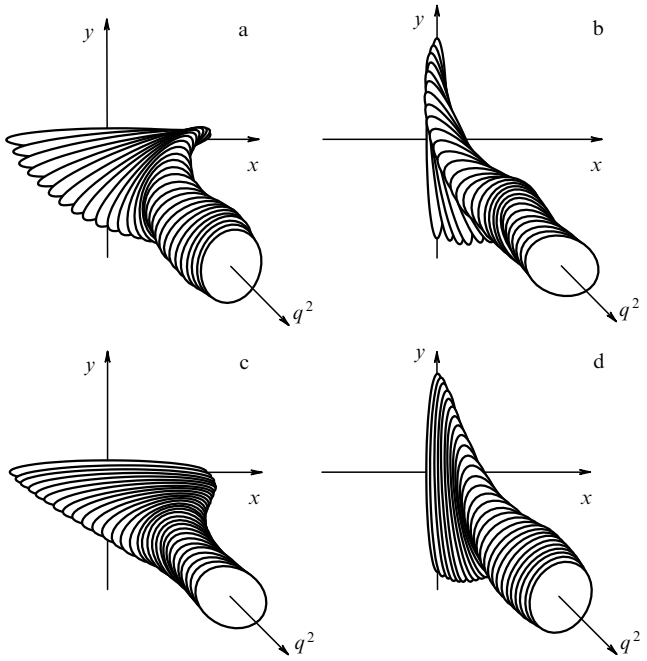

Figure 2. Uncertainty ellipses depending on the space frequency q of contributions to the field strength in the squeezed state: for field $S_1(\boldsymbol{\rho}, t)$ (a) before and (c) after the compensation for diffraction with a thin lens; (b, d) same for field $S_2(\boldsymbol{\rho}, t)$. The squeezing factor is $\exp\bigl(r(0,0)\bigr) = 3$.

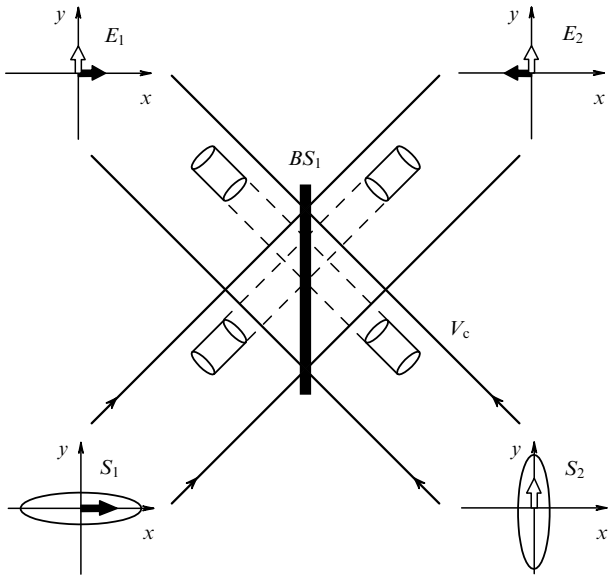

Figure 3. Production of EPR fields by optical mixing of fields in the squeezed state.

part of the diagram. The squeezing is assumed to be efficient; therefore, the main contribution comes from the extended quadrature components of the field strengths, whereas the squeezed components are small and are not shown in the diagram. The strengths of the scattered fields $E_1(\boldsymbol{\rho}, t)$ and $E_2(\boldsymbol{\rho}, t)$ in the corresponding coherence volumes can be obtained by the vector summation of the field strengths $S_1(\boldsymbol{\rho}, t)$ and $S_2(\boldsymbol{\rho}, t)$ in the squeezed state (see top of Fig. 3). We see that, in the limit of effective squeezing, the scattered fields have the same (up to a sign) quadrature components, and are therefore completely correlated.

Quantum calculations indicate that the resulting EPR correlations have the following features.

(1) The values of the EPR fields $E_1(\boldsymbol{\rho}, t)$ and $E_2(\boldsymbol{\rho}, t)$ are correlated in the corresponding coherence volumes.

(2) The effective correlations have space and time scales of S_c and T_c — that is, they occur for the field strengths averaged over the coherence volume. Fields averaged over small volumes $V \ll V_c$ feature independent fluctuations.

(3) As the squeezing increases, the EPR correlations increase, as does the mean number of photons of squeezed light in the coherence volume. In the case of continuous variables, ideal EPR correlations call for arbitrarily large energy expenditures.

For teleportation — that is, for the reproduction of the quantum state of the object field in the reconstructed field, the transmission coefficient of the classical channel

$$A_{\text{in}}(\boldsymbol{\rho}, t) \to I_{x,y}(\boldsymbol{\rho}, t) \to A_{\text{out}}(\boldsymbol{\rho}, t)$$

should be put equal to 1. Then the quadrature components of the EPR field strength $E_1(\boldsymbol{\rho}, t)$ pass into the output field with transfer coefficients of ± 1 (here we should take into account the phase gain introduced by the beam splitter BS_2). As indicated above, the reflectivity of the exit mirror M for the EPR field $E_2(\boldsymbol{\rho}, t)$ is assumed to be close to 1. For the teleported field, we obtain

$$A_{\text{out}}(\boldsymbol{\rho}, t) = A_{\text{in}}(\boldsymbol{\rho}, t) + F(\boldsymbol{\rho}, t)\,, \tag{7}$$

where

$$F(\boldsymbol{\rho}, t) = E_2(\boldsymbol{\rho}, t) + E_1^{\dagger}(\boldsymbol{\rho}, t) \tag{8}$$

is the contribution of the quantum fluctuations introduced by the EPR fields. In the unattainable ideal case, this contribution would be arbitrarily small because of the mutual cancellation of the correlated quadrature amplitudes of the contributions $E_2(\boldsymbol{\rho}, t)$ and $E_1^{\dagger}(\boldsymbol{\rho}, t)$ that have passed into the teleported field via the classical and the quantum channel. It is the compensation of quantum correlations that distinguishes quantum holographic teleportation from classical holography. For a more realistic case of finite squeezing, a quantum analysis [9–11] indicates that the noise field $F(\boldsymbol{\rho}, t)$ is classical and features Gaussian statistics. The noise correlation functions for different points in time and space differ significantly from zero if these points belong to the same coherence volume.

To clarify the meaning of the space–time scales and the role of averaging of the field strength, let us find the quadrature amplitudes of the field $A_{\text{out}}(\boldsymbol{\rho}, t)$ averaged over a space region (pixel) of area $S = \Delta^2$, and over the sampling time T:

$$X_{\text{out}}(j, i) = \frac{1}{\sqrt{ST}} \int_{S_j} \mathrm{d}\boldsymbol{\rho} \int_{T_i} \mathrm{d}t \left(A_{\text{out}}(\boldsymbol{\rho}, t) + A_{\text{out}}^{\dagger}(\boldsymbol{\rho}, t) \right), \tag{9}$$

$$Y_{\text{out}}(j, i) = \frac{\mathrm{i}}{\sqrt{ST}} \int_{S_j} \mathrm{d}\boldsymbol{\rho} \int_{T_i} \mathrm{d}t \left(A_{\text{out}}(\boldsymbol{\rho}, t) - A_{\text{out}}^{\dagger}(\boldsymbol{\rho}, t) \right); \tag{10}$$

and similarly for $A_{\text{in}}(\boldsymbol{\rho}, t)$. Here, (j, i) is the discrete index that numbers the area and the averaging-time interval. We define the mean quadrature amplitudes of the noise field $F(\boldsymbol{\rho}, t)$ in a way similar to (9), (10) and denote them as $\mathcal{X}(j, i)$, $\mathcal{Y}(j, i)$. These amplitudes obey the Gaussian statistics given by the correlation matrix

$$\mathcal{C}(j, j'; i, i') = \langle \mathcal{X}(j, i)\, \mathcal{X}(j', i') \rangle = \langle \mathcal{Y}(j, i)\, \mathcal{Y}(j', i') \rangle\,. \tag{11}$$

The light fields in the squeezed state that are generated in one pass across the nonlinear crystal are broadband and have a short coherence time. If the sampling time is long enough ($T \gg T_c$), the noise fields on different time intervals are independent:

$$\mathcal{C}(j, j'; i, i') = \delta_{i,i'}\, \mathcal{C}(j, j')\,. \tag{12}$$

If the sampling areas are large compared with the coherence area ($S \gg S_c$), then the noise fields on different areas are also independent:

$$\lim_{S/S_c \to \infty} \mathcal{C}(j, j') = 2\delta_{j,j'} \exp\bigl(-2r(0, 0)\bigr)\,. \tag{13}$$

The limit of classical holography corresponds here to the absence of squeezing, $r(0, 0) = 0$, while in the case of effective generation of EPR fields in the quantum channel we have $r(0, 0) \gg 1$, and the contribution from the noise field disappears.

Various criteria of the closeness of the quantum states of the input and the teleported field have been proposed [19]. The efficiency of teleportation of the quantum state is often characterized by fidelity, which, for a pure state, is defined as

$$F = \left| \langle \psi_{\text{in}} | \psi_{\text{out}} \rangle \right|^2. \tag{14}$$

However, in the case of the teleportation of a light field distributed in space and time, such a definition runs into a fundamental difficulty. This difficulty is associated with the nature of the field as a system with a large number of degrees of freedom, and can be understood from the following simple consideration. Let the fidelity of the quantum teleportation of the state of the field confined within a certain space–time region be less than unity by a small but finite increment. If we now consider a system with the parallel teleportation of many volumes of the field in the same state, then the fidelity defined according to (14) equals a high power of the fidelity found earlier — that is, in the limit of a large system, it will always be zero. In this way, in the case of quantum holographic teleportation, one should use not the fidelity defined by (14) (which may be referred to as 'global fidelity'), but rather the reduced fidelity defined for the reduced set of degrees of freedom that is of interest for us.

If we assume that, in our example, the relevant degrees of freedom correspond to $n = 1, 2, \ldots$ volumes of averaging (pixels) as defined above, then, for the important special case of the input field $A_{\text{in}}(\boldsymbol{\rho}, t)$ in the multimode Glauber coherent state, quantum calculations yield [11]

$$F_n = \frac{1}{\det\left\{\delta_{i,j} + (1/2)\mathcal{C}(i,j)\right\}}\,. \tag{15}$$

Hence we see that the fidelity of teleportation of the quantum-field state for n pixels depends on both their number and the correlations of the noise field on the pixels of interest. The correlations lose their importance if the area of averaging S is much larger than the coherence area S_c and the correlation matrix becomes diagonal. Then, as in the case of a spatially single-mode field, quantum holographic teleportation exhibits high fidelity with efficient squeezing and deep EPR correlations in the quantum channel.

The authors acknowledge the support of Network QUANTIM, the IST program of the European Union.

References

1. Bouwmeester D, Ekert A K, Zeilinger A (Eds) *The Physics of Quantum Information* (New York: Springer, 2000)
2. Kilin S Ya *Usp. Fiz. Nauk* **169** 507 (1999) [*Phys. Usp.* **42** 435 (1999)]
3. Bennett C H et al. *Phys. Rev. Lett.* **70** 1895 (1993)
4. Kwiat P G et al. *Phys. Rev. Lett.* **75** 4337 (1995)
5. Bouwmeester D et al. *Nature* **390** 575 (1997); Boschi D et al. *Phys. Rev. Lett.* **80** 1121 (1998)
6. Vaidman L *Phys. Rev. A* **49** 1473 (1994); Braunstein S L, Kimble H J *Phys. Rev. Lett.* **80** 869 (1998)
7. Furusawa A et al. *Science* **282** 706 (1998)
8. Van Loock P, Braunstein S L, Kimble H J *Phys. Rev. A* **62** 022309 (2000); quant-ph/9902030
9. Sokolov I V et al. *Opt. Commun.* **193** 175 (2001)
10. Sokolov I V et al., quant-ph/0007026
11. Gatti A et al. (in preparation)
12. Braunstein S L *Opt. Photon. News* (Jan.) 10 (1999)
13. Kolobov M I, Sokolov I V *Zh. Eksp. Teor. Fiz.* **96** 1945 (1989) [*Sov. Phys. JETP* **69** 1097 (1989)]
14. Kolobov M I, Sokolov I V *Phys. Lett. A* **140** 101 (1989)
15. Kolobov M I, Sokolov I V *Europhys. Lett.* **15** 271 (1991)
16. Kolobov M I *Rev. Mod. Phys.* **71** 1539 (1999)
17. Brambilla E et al., quant-ph/0010108
18. Kolobov M I *Phys. Rev. A* **44** 1986 (1991)
19. Ralph T C, Lam P K *Phys. Rev. Lett.* **81** 5668 (1998)

PACS numbers: 32.70.Fw, 32.70.Jz, 42.25.Hz, 42.25.Gy, 42.50.Gy
DOI: 10.1070/PU2001v044n11ABEH000988

Action of optical radiation on the boundary of a rarefied resonant medium. New possibilities and problems

T A Vartanyan

The reflection of resonant optical radiation from the boundary of a gaseous medium has long been considered a trivial illustration of the laws of physical optics [1]. The use of this effect for studying the interactions of atoms with one another and with the solid surface became possible only after the experimental discovery [2] and theoretical interpretation [2, 3] of narrow resonances in reflection spectra, free of Doppler broadening. First of all, the resonant collisional broadening in the centers of atomic lines, inaccessible to the standard absorption spectroscopy because of self-absorption effects in optically dense atomic vapors, was determined [4]. The constants of the Van der Waals interaction between a solid surface and a resonantly excited atom, for which other measurement techniques are not known, were also measured [5]. At the same time, inadequacies of the theoretical treatment gave rise to certain problems and paradoxes with interpreting experimental data without proper account for such attendant circumstances as the nonexponential absorption in the medium, deviation of the local field from the mean field, the saturation of atomic transitions, and the interplay of various factors causing shifts, broadening, and deformation in the spectral contours of the lines of selective mirror reflection.

This communication deals with solving certain theoretical problems that impede the more extensive use of the diagnostic capabilities of the reflection spectroscopy of rarefied gaseous media. Special attention will be paid to the nonlinear optical processes associated with the reflection of resonant optical radiation from the boundary of a rarefied gaseous medium [6] and effects of the second order with respect to the optical density of the medium.

A specific feature of rarefied resonant gas as a dispersive optical medium is that, even though the proper geometric dimensions of the atom are small compared to the radiation wavelength, the response of an atom is essentially nonlocal if the free path of the atom without changes in polarization exceeds the radiation wavelength. This condition is equivalent to requiring that the Doppler broadening of the resonant transition in the atom be greater than its homogeneous width. The latter is the sum of the radiation and the collisional width. The radiation width of an allowed optical transition is about 10 MHz, which is much less than the characteristic magnitude of the Doppler broadening (500 MHz). Therefore, the Doppler broadening exceeds the homogeneous width right up to concentrations of order $10^{14}\,\text{cm}^{-3}$. For higher concentrations, the resonant transmission of excitation upon the collision of an excited atom with a nonexcited one reduces the free path of the atom without changes in polarization to a value that is less than the wavelength of the radiation resonant to the atomic transition. In this case, the polarization of the atom is mainly determined by the field acting upon the atom at the point where the atom is currently located. If, however, the concentration is less than $10^{14}\,\text{cm}^{-3}$, the optical response of the resonant gas is essentially nonlocal.

The description of homogeneous media with a nonlocal response mainly consists in taking into account the spatial dispersion of the dielectric permittivity. Then the propagation of additional light waves becomes possible in the medium. The ordinary boundary conditions are not sufficient to calculate the coefficients of reflection and transmission at the boundary of such a medium, and it becomes necessary to formulate additional boundary conditions. A similar situation has been considered in detail in the optics of crystals [8]. In the case of a rarefied resonant gas, the additional solutions of the dispersion equation correspond not to propagating waves but rather to heavily damped waves whose contributions can be neglected. The spatial structure of the main wave is then very complicated and does not reduce to a simple exponential dependence on the coordinates. The additional boundary conditions that should be specified to determine this structure have the simple microscopic meaning of the initial polarization of atoms bounced off the wall that confines the gas, but they can hardly be formulated in macroscopic terms.

If the field inside the medium does not vary exponentially, the concept of the refractive index becomes meaningless. Nevertheless, the coefficient of reflection for normal incidence can be calculated using the conventional Fresnel formulas with the refractive index replaced by the surface admittance of the gas defined by analogy with the anomalous skin effect in metals, as the logarithmic derivative of the field at the boundary divided by the wave number and the imaginary unit. The surface admittance can be calculated using the Maxwell – Bloch set of equations [9]. In the conventional theory of dispersion, the coordinate dependence of the field is assumed to be exponential, and the motion of atoms is taken into account by inclusion of the Doppler shift of the resonant frequency in the expression for the steady-state polarization of the atom. If the Doppler broadening is strong, the polarization of the majority of the atoms that have bounced off the boundary reaches a steady state at distances from the boundary that are much larger than the wavelength. The replacement of the actual behavior of the polarization in the surface layer of such a considerable thickness with the steady-state polarization leads to essentially wrong results. The proper approach consists in solving the set of Maxwell – Bloch equations with due account for the boundary conditions for the density matrix of the atoms that bounce off the boundary. In most cases, we can assume that a collision with the surface completely quenches the electron excitation [10], so that the atom recedes from the boundary in the electron ground state. The boundary condition for atoms approaching the boundary consists in delimiting the polarization at large distances from the boundary. In the first order with respect to the optical density of the gas, this condition is equivalent to taking into account only the steady-state polarization of the atoms approaching the boundary. In Fig. 1, the shape of the spectral line of the selective mirror reflection from the boundary of a rarefied resonant gas (curve *1*) is compared with the results of the conventional theory of dispersion, obtained without taking into account the transient process of the establishment of the steady-state polarization of the reflected particles (curve *2*). In the region of anomalous dispersion of vapor, instead of a odd contour corresponding to the variation of the refraction index in a Doppler-broadened gas, we can see a narrow peak of the reflection coefficient free of Doppler broadening. The reason for such a sharp change in the shape of the reflection line is

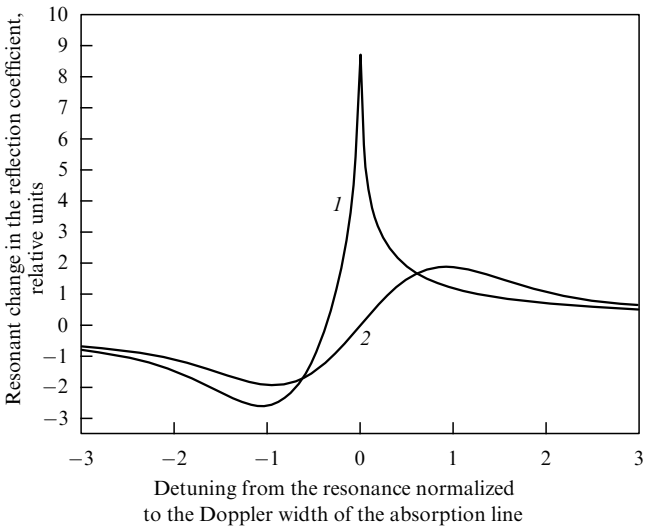

Figure 1. Spectral contour of a resonance, free of Doppler broadening, in the reflection spectrum from the glass – rarefied gas interface in the region of anomalous dispersion. The Doppler width is 100 times the homogeneous linewidth (curve *1*). For comparison, curve *2* represents the result of the conventional theory of dispersion neglecting the transient process of the establishment of the steady-state polarization of the particles that bounce off the interface.

that, on account of the transient process of the establishment of the steady-state polarization, the receding particles do not give a resonant contribution to the blue wing of the line, where it could be expected in accordance with the sign of the Doppler frequency shift. At the same time, in the red wing of the line, where the polarization amplitude of the reflected particles does not exhibit any resonance-specific features, the contribution of the particles that bounce off the boundary to the coefficient of reflection exhibits a resonant increase because the spatial structure of the transient polarization precisely matches the spatial structure of the reflected wave. The steady-state polarization of the atoms approaching the boundary exhibits a resonant increase in the red wing of the absorption line in complete agreement with the sign of the Doppler frequency shift. Thus, the receding atoms that are seeking a steady polarization state give exactly the same contribution to the coefficient of reflection as the atoms in the steady state that approach the boundary with an equal and oppositely directed velocity. As a result, averaging over velocities effectively reduces to the integration over one half of the Maxwell distribution, corresponding to the velocities of only the approaching particles. Such an abrupt termination of the velocity distribution at zero velocity gives rise to a narrow peak in the reflection coefficient.

If the resonant gas forms a thin layer between two dielectric media, we encounter two new circumstances at once. Firstly, the polarization of the atoms approaching the front boundary does not have time to reach a steady value after being bounced off the rear boundary, and secondly, the collision with the rear boundary leads to the quenching of polarization for atoms with velocities of either sign. The shape of the spectral reflection line depends in this case on the thickness of the gas layer. If the thickness of the layer is one and a half times the wavelength, we see a even spectral contour, and the amplitude of the field reflected from the thin layer is four times larger than that of the field reflected from a thick layer [11].

If the saturation effects are taken into account, the atoms moving in opposite directions give different contributions to the coefficient of reflection. If the longitudinal and the transverse relaxation time differ considerably, then the power of saturation is considerably different for atoms approaching the boundary and atoms receding from the boundary [12]. The relatively low power of radiation at which the saturation effect becomes noticeable for the reflection of resonant radiation from the boundary of rarefied vapor, facilitates the use of such a boundary [13] and a narrow layer of vapor [14] for nonlinear optical control of light beams, and for image processing. The transient process of the establishment of the steady-state polarization and population difference for the energy levels of the atoms receding from the boundary also leads to the appearance of longitudinal periodic structures near the reflecting surface. Of special interest is the possibility of controlling the period and depth of oscillations in the population difference by adjusting the intensity or frequency of radiation [15].

In the first order with respect to the optical density of the vapor, the maximum of the narrow Doppler-free contour of the selective mirror reflection coincides with the frequency for the transition in an isolated atom. However, a more efficient use of the diagnostic capabilities of selective reflection requires calculating the position of the maximum at least to terms quadratic with respect to the density of the gas. Such a calculation poses considerable mathematical difficulties because the boundary conditions for the atoms moving in opposite directions are posed in different regions. The exact solution obtained in Ref. [3] using the Wiener–Hopf method is very cumbersome, and can hardly be extended to more complicated cases. We succeeded in developing a simpler method that allows the calculation of the coefficient of reflection in the second order with respect to the optical density of the medium. The explicit analytical expression for the shift of the reflection maximum [16] implies that this shift is proportional to the product of the densities of the atoms moving in opposite directions. This circumstance, as well as the above-mentioned easy saturation of the particles approaching the boundary, explains the experimentally noted absence of a strong blue shift of the reflection maximum predicted in Ref. [3]. The same method was used to express the analytical correction to the position of the reflection maximum due to the deviation of the local field from the mean field [17]. The magnitude of this correction greatly exceeds the estimates derived from the intuitive physical assumption of the smallness of the Lorentz–Lorenz correction in a nonuniformly broadened medium [18], and helps to understand the earlier numerical results [19].

The narrow resonances of selective mirror reflection will certainly find wide practical application, and will be used to study various physical processes on the gas–solid interface, to which they are extremely sensitive. In this context, the further development of the theory, which will help in extracting much information about the processes on and near the surface and also give an adequate description of devices based on the effect of selective reflection from rarefied resonant vapor, seems very expedient [20].

The author is grateful to A M Bonch-Bruevich for his continued support at all stages of this work. Some of the results presented here were obtained with the financial support of the Russian Foundation for Basic Research and the State Program 'Fundamental Metrology'.

References

1. Wood R W *Philos. Mag.* **18** 187 (1909)
2. Cojan J L *Ann. Phys.* (Paris) **9** 385 (1954)
3. Schuurmans M F H *J. Phys.* (Paris) **37** 469 (1976)
4. Akul'shin A M et al. *Pis'ma Zh. Eksp. Teor. Fiz.* **36** (7) 247 (1982) [*JETP Lett.* **36** 303 (1982)]
5. Oria M et al. *Europhys. Lett.* **14** 527 (1991)
6. Vartanyan T A *Zh. Eksp. Teor. Fiz.* **88** 1147 (1985) [*Sov. Phys. JETP* **61** 721 (1985)]
7. Vartanyan T A *Opt. Spektrosk.* **70** 257 (1991) [*Opt. Spectrosc.* **70** 147 (1991)]
8. Agranovich V M, Ginzburg V L *Kristallooptika s Uchetom Prostranstvennoĭ Dispersii i Teorii Eksitonov* 2nd ed. (Crystal Optics with Spatial Dispersion, and Theory of Excitons) (Moscow: Nauka, 1979) [Translated into English (Berlin: Springer-Verlag, 1984)]
9. Allen L, Eberly J *Optical Resonance and Two-level Atoms* (New York: Wiley, 1975) [Translated into Russian (Moscow: Mir, 1978)]
10. Przhibel'skiĭ S G, Khromov V V *Opt. Spektrosk.* **88** 22 (2000) [*Opt. Spectrosc.* **88** 17 (2000)]
11. Vartanyan T A, Lin D L *Phys. Rev. A* **51** 1959 (1995)
12. Vartanyan T A *Opt. Spektrosk.* **68** 625 (1990) [*Opt. Spectrosc.* **68** 365 (1990)]
13. Akul'shin A M et al. *Opt. Spektrosk.* **66** 723 (1989)
14. Vartanyan T A, Lin D L *Eur. Phys. J. D* **1** 217 (1998)
15. Vartanyan T A *Opt. Spektrosk.* **88** 624 (2000) [*Opt. Spectrosc.* **88** 564 (2000)]
16. Vartanyan T A, Bloch D, Ducloy M *AIP Conf. Proc.* **328** 249 (1995)
17. Vartanyan T A, Weis A *Phys. Rev. A* **63** 063813 (2001)
18. Vuletic V et al. *Opt. Commun.* **99** 185 (1993)
19. Guo J et al. *Opt. Commun.* **110** 197 (1994)
20. Müller R, Weis A *Appl. Phys. B* **66** 323 (1998)